

Scientific paper

# Determination of the Interactions Between $Zn^{2+}$ and Water Soluble Polymer Ligands with Potential Use in Controlled Drug Delivery

Nada Verdel,<sup>1,\*</sup> Andrej Kržan,<sup>2</sup> Mojca Benčina<sup>2</sup> and Majda Žigon<sup>2</sup><sup>1</sup> Faculty of Chemistry and Chemical Technology, University of Ljubljana, Askerceva 5, 1000 Ljubljana, Slovenia<sup>2</sup> National Institute of Chemistry, Hajdrihova 19, 1000 Ljubljana, Slovenia

\* Corresponding author: E-mail: nadaverdel@gmail.com

Received: 28-01-2013

## Abstract

Biodegradable copolymers of aspartic and lactic acids were synthesized for potential use in controlled drug release. The proportion of aspartic acid moieties in the copolymers was 0.9 and 0.1, the molecules were partially branched and had absolute molar masses over 100,000 g/mol. The drug could be attached to the copolymer via metal (particularly zinc) ions, so a method to estimate the interactions between zinc ions and the water-soluble polymers by fluorescence spectroscopy was developed. The stability constants of binding of zinc and the concentrations of zinc bound to polymer were determined. The results confirm that zinc ions at pH 6 preferentially bind to side groups of aspartic acid units of the copolymers.

**Keywords:** Polyamino acid, controlled drug delivery, biodegradable carrier, fluorescence spectroscopy, zinc, polymer coordination compound.

## 1. Introduction

This study focused on biodegradable polymers that can potentially be used for pharmaceutical purposes in controlled drug release. Polymers as drug carriers are used in two types of delivery systems, colloidal carriers and polymer-drug conjugates. In colloidal formulations, the polymer encapsulates drug within micro- or nanoparticles.<sup>1</sup> In polymer-drug conjugates, the drug is covalently bound to the polymer.<sup>2</sup> For such purposes, the drug could be attached to the polymer via dative covalent bonds or coordinate bonds with metal ions like zinc, and for the polymer components lactic and aspartic acid moieties could be combined.

Poly(aspartic acid), PA, is a typical hydrophilic biodegradable polymer with aspartic acid monomer units. The most common method for the synthesis of PA involves the polycondensation of aspartic acid into polysuccinimide, followed by its hydrolysis to sodium polyaspartate. The hydrolyzed form, sodium polyaspartate, has hydrophilic carboxylate side groups that can interact with metal ions.<sup>3</sup> It degrades quickly under physiological and

biological conditions. However, it is insoluble in organic solvents and does not have thermoplastic properties, which makes it difficult to obtain PA films or mouldings; it can only be processed as an aqueous solution or in a hygroscopic powder form.<sup>4</sup>

On the other hand, polylactide or poly(lactic acid), PLA, is one of the most intensively studied biodegradable thermoplastic polymers and contains lactic acid monomer units. PLA is hydrophobic and soluble in organic solvents. It is currently used in a number of biomedical applications, such as sutures or fibres,<sup>5</sup> stents, implants for bone fixation<sup>6</sup> and drug delivery devices.<sup>7</sup> It is also being evaluated as a material for tissue engineering.<sup>8</sup> One of the shortcomings of this polymer is that there is no pendant functional group on the backbone.

One of the possibilities to combine the advantages of both PLA and PA derivatives is to make amphiphilic copolymers.<sup>4</sup> PA can bind metal ions and is water-soluble,<sup>9</sup> whereas PLA has good mechanical properties and dissolves in organic solvents. By changing the ratio of aspartic and lactic acid units we can therefore obtain amphiphilic copolymers to which a drug could be attached via zinc ion bridges. For many years zinc has been used to treat

epithelial disorders, ranging from wound healing to diarrhea and ulcerative colon disease.<sup>10</sup> It is found in all body tissues, with ~85% of the whole body zinc in muscle and bone, and another 11% found in the skin and liver.<sup>11</sup> Typically, humans appear to have the capacity to regulate whole body zinc content over a ten-fold change in intake.<sup>12</sup>

Zinc ions bind to copolymers of aspartic and lactic acids to form polymer coordination compounds. In polymer coordination compounds metal ions interact with ligand groups situated on the polymer chains. The kind and strength of the metal ion to ligand interaction can be described by stability constants. Stability constants of polymer coordination compounds can be calculated with the help of many theoretical models. For our system, the most suitable model is described by Flory's concept of infinitely large polymer chains.<sup>13,14</sup>

In this paper we report a method of determining the interactions between polymer ligands and  $Zn^{2+}$  in aqueous solutions by fluorescence spectroscopy. To determine the concentration of free zinc, a fluorescent indicator that enables minimal interference with the equilibrium of zinc, was used. As zinc carriers copolymers of aspartic and lactic acids were prepared and the properties of the copolymers for potential use as carriers in chemically controlled drug release were characterized.

## 2. Experimental

### 2.1. Materials

L-aspartic acid (> 98%), L-lactic acid (> 85%), L-lactide – the cyclic dimer of lactic acid (98%), N,N-dimethylformamide (p. a., 99%) and lithium bromide, LiBr, (> 99%), purchased from Aldrich, N,N-dimethylacetamide, DMAc, (99%), purchased from Merck and zinc chloride (p. a., 98+%), purchased from Fluka, were used as received. Benzoylated dialysis tubing with pore size of  $\leq 1,200$  g/mol was purchased from Sigma Aldrich. Sodium poly( $(\alpha,\beta)$ -D,L-aspartate) (40 w.%) was purchased from Aldrich, with FTIR:  $\nu = 2600\text{--}3600$  (N-H and O-H), 1598 (C=O, carboxylate), 1648 (amide I), 1240 (amide III), 670 (amide V), 2867 and 2930 (C-H and  $CH_2$ ) and  $3086\text{ cm}^{-1}$  ( $-HC=$ , maleamic acid) and  $^1H$  NMR (in  $D_2O$ ):  $\delta = 4.7$  ( $\alpha$ -CH), 4.5 ( $\beta$ -CH), 2.76 ( $\beta$ - $CH_2$ ) and 2.65, 2.55 ppm ( $\alpha,\beta$ - $CH_2$ ). The degree of ionization according to Saudek<sup>15</sup> was 1. The fluorescent dye Fluozin-1, N-(2-methoxyphenyl)iminodiacetic

acid indicator, "cell impermeant", purchased from Molecular Probes, was dissolved in twice deionized Milli-Q water and kept protected from light at  $-20\text{ }^\circ\text{C}$ . 8 g of N-(carbamoylmethyl)iminodiacetic acid buffer (ADA) ( $K_d(Zn^{2+}) = 127\text{ nmol/L}$  at an equimolar ratio of  $Zn^{2+}$  and ADA,  $20\text{ }^\circ\text{C}$ , pH 7 and ionic strength 0.1 mol/L), purchased from Sigma, was dissolved in 50 mL 1 N NaOH.

### 2.2. Syntheses

Poly(succinimide-co-lactic acid), PSL, copolymers were synthesized in a 100-mL glass flask that was degassed by continuous degassing and back-filling with argon, except during the third step of synthesis when a vacuum pump was applied (Table 1). The reaction mixture consisted of aspartic acid and lactic acid or lactide without addition of catalysts or solvents. ALa copolymers were synthesized by reaction of aspartic and lactic acids, and ALt copolymers with aspartic acid and lactide. The reactions proceeded similarly to the procedure with aspartic acid and lactide reported by Shinoda et al.<sup>4</sup> under the reaction conditions summarized in Table 1. Upon heating the reaction mixtures changed into viscous liquids, which were very difficult to stir. At the end of the syntheses the reaction flask was taken out of the oil bath and cooled to  $45\text{ }^\circ\text{C}$ . The products were purified by dissolution in the minimal quantity of DMF and the filtrate was poured into distilled water to precipitate the polymer. The yellowish white polymer powder was dried for 12 hours at  $80\text{ }^\circ\text{C}$  in an oven. FTIR (KBr):  $\nu = 1750$  (C=O, ester), 1790, 1720 (C=O, succinimide), 1660–1630 (amide I), 1550–1530 (amide II), 1290–1260 (amide III), 640 (amide V), 3700–3000 (N-H and O-H), 2990–2945 (C-H and  $CH_2$ , stretching vibrations), 1130 (C-O, ester) and  $1400\text{ cm}^{-1}$  ( $CH_2$ , deformational vibrations).

In the next step, amphiphilic poly(sodium  $\alpha,\beta$ -aspartate-co-lactic acid) (PAL) copolymers were prepared by hydrolyses of cyclic succinimide rings to more hydrophilic aspartic acid units bearing carboxylate groups. The hydrolysis were performed with 1 M NaOH added dropwise. The products were purified by three days of dialysis with exchanging distilled water twice per day where compounds with  $\leq 1,200$  g/mol were separated from compounds having molecular weight over 2,000 g/mol. FTIR (KBr):  $\nu = 1600$  ( $COO^-$ , carboxylate), 3400 (N-H and  $NH_2$ ), 1240 (amide III) and  $670\text{ cm}^{-1}$  (amide V).

**Table 1:** Reaction conditions for the synthesis of copolymers of aspartic (A) and lactic acid (La) or lactide (Lt)

| sample | N | A  | La | Lt  | A/La <sub>feed</sub> | temperature ( $^\circ\text{C}$ ) / time (h) |                     |                                      |                              |
|--------|---|----|----|-----|----------------------|---|---------------------|--------------------------------------|------------------------------|
|        |   |    |    |     |                      | I. step<br>melting                          | II. step<br>cooling | III. step<br>vacuum ( $\sim 4$ mbar) | IV. step<br>further reaction |
| AM     | 4 | 16 | 17 | /   | 0.95                 | 180 / 2.5                                   | 180–40 / 0.5        | 40 / 0.3                             | 180 / 2.5                    |
| AL     | 3 | 42 | /  | 245 | 0.17                 | 180 / 2.5                                   | 180–160 / 0.5       | 160 / 18                             | /                            |

N = number of parallels, A/M<sub>feed</sub> = feed molar ratio

## 2. 3. Characterization Methods

Fourier transform infrared spectroscopy, FTIR, was carried out with a Perkin-Elmer 1725X FTIR spectrometer. Typical FTIR spectra were obtained using KBr pellets or FTIR spectra in aqueous solutions using AgCl plates, resolution 4-cm<sup>-1</sup>, range 400–4500 cm<sup>-1</sup>, 20 °C and with 10 scans for dry or 300 scans for aqueous samples.

Nuclear magnetic resonance, NMR, spectra were recorded on a VXR 300 Varian spectrometer. The solvent for PSL was deuterated dimethyl sulfoxide, DMSO-*d*<sub>6</sub> and the solvent for PAL was D<sub>2</sub>O with addition of a standard, (CH<sub>3</sub>)<sub>3</sub>SiCH<sub>2</sub>CH<sub>2</sub>CH<sub>2</sub>SO<sub>3</sub>Na, DSS at a temperature of 25 °C and a pulse angle of 90°. Acquisition parameters for <sup>1</sup>H NMR spectra were 300 MHz, 35 scans and 5-s relaxation time, and for <sup>13</sup>C NMR spectra 75 MHz, 30,000 scans and 2-s relaxation time.

Differential scanning calorimetry, DSC, was conducted on a Perkin Elmer DSC-7 in the temperature range from –60 to 200 °C at a heating and cooling rate of 20 and 200 °C/min, respectively.

Size exclusion chromatography with a detector for multiple angle light scattering, SEC-MALS, was conducted on a Dawn-DSP detector, laser photometer (He-Ne laser, λ<sub>0</sub> = 633 nm), Optilab-DSP differential refractometer (Wyatt Technology Co.), Perkin Elmer Series 200 pump and a PL Gel Mixed D 5 μm column with pre-column (Polymer Laboratories, Ltd.), with N,N-dimethyl acetamide (DMAc) containing lithium bromide (0.1 M) as mobile phase. The nominal flow rate of eluents was 0.8 mL/min. The mass of the samples injected onto the column was typically 0.1–0.2 mg. Data acquisition and evaluation utilized Astra 4.73.04 software (Wyatt Technology). The method is described in detail in Gričar et al.<sup>16,17</sup>

## 2. 4. Interactions Between Polymer Ligands and Zn<sup>2+</sup>

The interactions between polymer ligands and metal ions can be deduced by different analytical methods. By means of chemical methods like elemental analysis the coordination number and atomic structure of polymer coordination compounds can be determined.<sup>14</sup> By physicochemical methods like potentiometric titration the stability constants and coordination numbers of metal ions can be deduced, whereas by conductometric titration the density of charge distribution, distribution of free metal ions, transport of total charged particles and the conductivity of polyelectrolyte solutions can be determined.<sup>18</sup> By spectroscopic methods like FTIR spectroscopy the molecular coordination structures, the position of coordination bonds on linear and crosslinked polymer chains, the special features of conformations, the shapes of functional groups and hydration layers can be defined. And by means of NMR spectroscopy the positions of metal ions on polymer ligands can be deduced.<sup>14</sup>

Above mentioned methods mostly demand a purified polymer coordination compound with no free metal ions in the solution. However, the equilibrium of free and bound Zn<sup>2+</sup> in aqueous solutions of the polymer ligands prevents complete removal of free Zn<sup>2+</sup>. The extent of the interactions between polymer ligands (L) and Zn<sup>2+</sup> was therefore determined by fluorescent spectroscopy where the addition of an appropriate fluorescence indicating dye permits minimal interference with the equilibrium. For this, the indicator FluoZin-1 was used and the resulting fluorescence intensity indicated the concentration of free Zn<sup>2+</sup> in the aqueous solution from which the concentration of bound Zn<sup>2+</sup> was calculated according to the equation [Zn<sup>2+</sup>]<sub>t</sub> = [Zn<sup>2+</sup>]<sub>f</sub> + [Zn<sup>2+</sup>]<sub>b</sub>.

FluoZin-1 is based on N-(2-methoxyphenyl)imino-diacetate chelator with stability constant for binding of Zn<sup>2+</sup>, K<sub>d</sub>(Zn<sup>2+</sup>) = 8 μmol/L. FluoZin-1 is designed for detection of Zn<sup>2+</sup> in the 0.05–50 μmol/L concentration range and exhibits a fluorescence intensity dependent on the concentration of free Zn<sup>2+</sup> with no accompanying spectral shift. According to the manufacturer's specification, the dissociation constant of FluoZin-1 is dependent on pH, temperature, ionic strength and viscosity of the solvent, the presence of other ions and compounds, photobleaching and the type of spectrofluorometer. Hence, it is important that all these factors are controlled or kept constant throughout the measurements.

The measurements by fluorescence spectroscopy were performed on a Perkin Elmer LS50 spectrofluorometer under the following conditions: emission range 500–550, excitation 490, automatic standard employment of photomultiplier, excitation slit 15 and emission slit 2.5 nm. Before a measurement was performed, the sample was thermostatted in the spectrofluorometer for 10 seconds at 20 °C. A 1 cm square quartz cuvette (0.5 mL) was used. The concentration of the indicator in the cuvette was 11.0 μmol/L and the ionic strength of the solution 0.1 mol/L. At the end of each experiment calibration was made by measurement of F<sub>min</sub>, a blank, and F<sub>max</sub>, the indicator saturation. Relative intensities of fluorescence, F\*, were calculated according to the manufacturer's specifications via Equation (1):

$$F^* = (F - F_{\min}) / (F_{\max} - F) \quad (1)$$

F denotes the fluorescence intensity of the sample. Each series of measurements were calibrated with the calibration curve (F\* = f([Zn<sup>2+</sup>]<sub>f</sub>)), where [Zn<sup>2+</sup>]<sub>f</sub> denotes the concentration of free Zn<sup>2+</sup>. The slope of the calibration curve of ZnCl<sub>2</sub> solutions, k, and F\* of solutions of ZnCl<sub>2</sub> + polymer ligands, L, were used to calculate [Zn<sup>2+</sup>]<sub>f</sub> in solutions of ZnL by Equation (2):

$$[Zn^{2+}]_f = k \cdot F^* \quad (2)$$

In spite of keeping the pH, temperature, ionic strength of the solvent and settings of the spectrofluoro-

meter constant, the slope of the calibration curve changed daily. The reason, among others, was the alteration of air humidity. Therefore the instrument was calibrated daily with a new calibration curve.

Photobleaching of the indicator was checked by measuring  $F$  of the solutions containing  $\text{ZnCl}_2 + \text{ADA}$  and altering the duration of indicator exposure to daylight and any radiation in the spectrofluorometer before measurement. The statistical errors for six and four replicate measurements of  $F$  of solutions of  $\text{ZnCl}_2 + \text{ADA}$  were calculated. Errors in  $F$ ,  $F_{\min}$  and  $F_{\max}$  measurements,  $dF^*/F^*$ , were calculated via Equation (3); where  $dF$  – standard deviation of  $F$ ,  $dF_{\min}$  – deviation of  $F_{\min}$ ,  $dF_{\max}$  – deviation of  $F_{\max}$ :

$$\frac{dF^*/F^*}{+ (dF_{\max} + dF) / (F_{\max} - F)} = \frac{(dF + dF_{\min}) / (F - F_{\min})}{(F - F_{\min})} \quad (3)$$

The interactions between  $\text{Zn}^{2+}$  and polymer ligands were determined by measuring  $[\text{Zn}^{2+}]_f$  in aqueous solutions of  $\text{ZnL}$  with PA, PAL ALa (90% A) and PAL ALt (10% A) at pH 6. The  $\text{ZnL}$  solutions were prepared by simply adding  $\text{ZnCl}_2$  ( $[\text{Zn}^{2+}]_t$ ) to the aqueous solutions of polymer ligands without further purification. By this, the exact  $[\text{Zn}^{2+}]_t$  was known. The measurements were carried out at constant  $[\text{Zn}^{2+}]_t$  of 20, 40, 60 and 80  $\mu\text{mol/L}$  on changing the total concentration of polymer ligand,  $[\text{L}]_t$ . The concentrations of PA, PAL ALa and PAL ALt were calculated by knowing the precise volume and weight of the solution and the molecular weight of the average (co)monomer unit,  $M_{n\text{-unit}}$ ;  $M_{n\text{-unit}}$  values were deduced by NMR spectroscopy. Two types of plots, describing linear dependence, were used:

- *Type 1*:  $[\text{PA}]_t = f(\ln[\text{Zn}^{2+}]_f)$ ,  $[\text{ALa}]_t = f(\ln[\text{Zn}^{2+}]_f)$  and  $[\text{ALt}]_t = f(\ln[\text{Zn}^{2+}]_f)$  at constant  $[\text{Zn}^{2+}]_t$ , where “ $t$ ” and “ $f$ ” denote total and free, respectively, (Figure 3),
- *Type 2*:  $[\text{Zn}^{2+}]_b/[\text{Zn}^{2+}]_f = f([\text{PA}]_t)$ ,  $[\text{Zn}^{2+}]_b/[\text{Zn}^{2+}]_f = f([\text{ALa}]_t)$  and  $[\text{Zn}^{2+}]_b/[\text{Zn}^{2+}]_f = f([\text{ALt}]_t)$ ; Figure 4.

The linear relationships in plots of *Type 1*,  $[\text{L}]_t = f(\ln[\text{Zn}^{2+}]_f)$ , describe the links between bound and total  $\text{Zn}^{2+}$  from which we could draw plots of *Type 2*. Plots of *Type 2* are Flory's equations for unidentate ligands, independent of their position on the polymer chain,  $[\text{Zn}^{2+}]_b/[\text{Zn}^{2+}]_f = K_L \cdot [\text{L}]_t - K_L \cdot [\text{L}]_b$ , where  $K_L$  denotes the stability constant of the binding of  $\text{Zn}^{2+}$  to L and  $[\text{L}]_b$  the concentration of bound polymer ligands.<sup>19</sup>

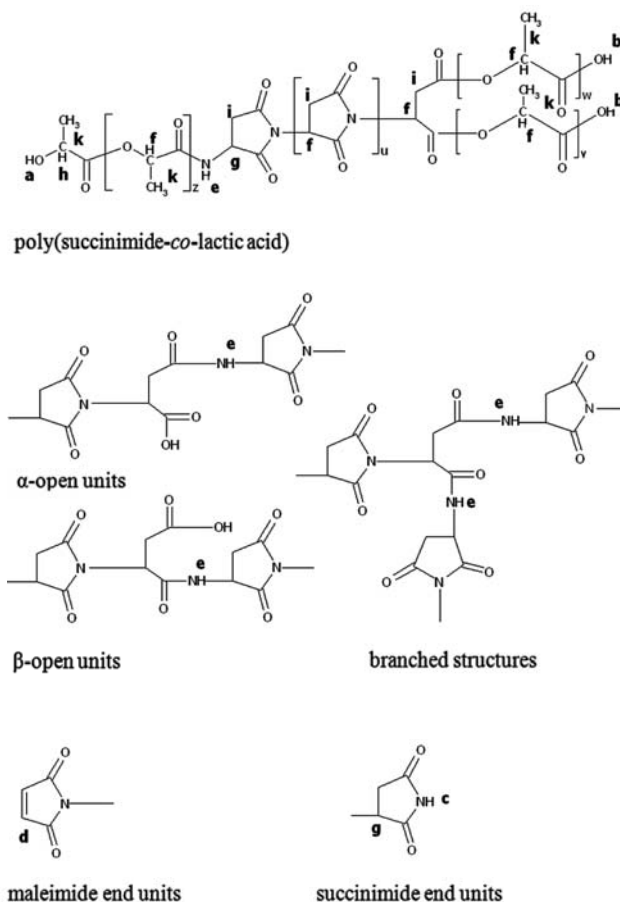
## 3. Results and Discussion

### 3.1. Synthesis and Characterization

Amphiphilic biodegradable copolymers with aspartic and lactic acid moieties were synthesized as described in the literature<sup>4</sup>, with some modifications in the preparation procedure. NMR and FTIR spectra show that under

the conditions (summarized in Table 1) poly(succinimide-*co*-lactic acid) (PSL) copolymers were synthesized. By basic hydrolysis of PSL poly(sodium ( $\alpha,\beta$ )-aspartate-*co*-lactic acid) (PAL) copolymers were prepared. Copolymers with a higher amount of aspartic acid, ALa, were synthesized from aspartic and lactic acid, and copolymers with a higher amount of lactic acid, ALt, from aspartic acid and lactide (Table 2). The PAL ALa copolymers were water-soluble, but insoluble in organic solvents, whereas PAL ALt were amphiphilic.

Throughout the hydrolysis of PSL to PAL, the ratio of comonomer units and end groups are preserved.<sup>20</sup> Maleimide end groups in PSL transform through hydrolysis to maleamic acids and due to the presence of double bonds between carbon atoms, form irregular structures in PSL as well as in PAL (Scheme 1). Succinimide end groups transform through hydrolysis to asparagine end groups and succinamic acid end groups, whereas carboxy and hydroxy end groups remain unchanged after hydrolysis.<sup>21</sup> Shortly, preservation of comonomer units, irregular structures and end groups throughout the hydrolysis were reasons the characterization of copolymers was discussed mainly via characterization of PSL (Table 2).



Scheme 1. Schematic structures of poly(succinimide-*co*-lactic acid) copolymers.

**Table 2.** Average characteristics of synthesized copolymers of aspartic and lactic acids ALa and ALt, where the mole ratios between aspartic and lactic acid moieties in the feed stock and in the copolymer are  $A/La_{\text{feed}}$  and  $A/La_L$ , the average molar masses of comonomer units are  $M_{\text{n-unit}}$  and the number of end comonomer units per copolymer chain and the percentage of end groups per copolymer are  $N_{\text{chain}}$  and  $N_C$ , respectively

| L   | N (l) | A/La <sub>feed</sub> (l) | N <sub>chain</sub> (l) | FTIR (CO)                   |                          | NMR                                |                    |                                 |                             | DSC                 |
|-----|-------|--------------------------|------------------------|-----------------------------|--------------------------|------------------------------------|--------------------|---------------------------------|-----------------------------|---------------------|
|     |       |                          |                        | (ester) (cm <sup>-1</sup> ) | (SI) (cm <sup>-1</sup> ) | A/La <sub>L</sub> <sup>a</sup> (l) | A <sup>a</sup> (%) | N <sub>C</sub> <sup>b</sup> (%) | M <sub>n-unit</sub> (g/mol) | T <sub>g</sub> (°C) |
| ALa | 4     | 0.95                     | 141                    | c                           | 1787<br>1718             | 8                                  | 90                 | 8±4                             | 94                          | 58 ± 5 <sup>d</sup> |
| ALt | 3     | 0.17                     | 390                    | 1759                        | 1723                     | 0.13                               | 10                 | 6 ± 2                           | 75                          | 15 ± 5              |

N = number of parallels, <sup>a</sup> = ± 10%, estimated from <sup>13</sup>C NMR spectra of PSL in DMSO-*d*<sub>6</sub>, <sup>b</sup> = ± 10%, percentage of end groups in copolymers, determined from <sup>1</sup>H NMR spectra of PSL in DMSO-*d*<sub>6</sub>, <sup>c</sup> = band overlapped by other bands; SI = succinimide, <sup>d</sup> = results of DSC measurements after first heating, because after T<sub>g</sub> the copolymers degrade.

The structure of PSL copolymers was elucidated by <sup>1</sup>H and <sup>13</sup>C NMR spectroscopy (Scheme 1) and the signals were consistent with Shinoda's NMR study<sup>4</sup> on the copolymers of aspartic and lactic acids, Matsubara's NMR studies<sup>22</sup> on thermally prepared polysuccinimides and Espartero's study<sup>23</sup> on low molecular weight poly(lactic acid)s. Two major resonances in the <sup>1</sup>H NMR spectra of PSL, corresponding to methyl (k) and methine groups (f, g, h), were observed at 1.6–1 ppm and 5.4–4 ppm, respectively (Scheme 1). The signal of water overlaps the signal of methylene protons. Therefore on addition of CF<sub>3</sub>COOH to the deuterized solvent containing dissolved PLS,<sup>4</sup> the residual water peak displayed a higher chemical shift (approx. 8.8 ppm) and the characteristic multiplets at 3.8–2.2 ppm were assigned to the methylene protons (i) of succinimide. The methine protons of succinimide (j) at 5.4–4.5 ppm overlap with the PLA methine resonances (f). Resonances at 9.3–7.6 ppm indicate amide protons (-CONH-) (e) in branched laurylamide structures and α-, β-succinimide open units. The small resonance at 7.05 ppm indicates the presence of maleimide end groups (d), that at 11.5 ppm succinimide end groups (c), and the resonances at 5.5 and 12–13 ppm -OH (a) and -COOH (b) lactic acid end groups, respectively.

<sup>13</sup>C NMR spectra (Figure 1) show signals of succinimide CO at 178–170 ppm, ester CO at 174–169 ppm and amide CO at 171–166 ppm. The lactic acid and succinimide CH were assigned to 72–67 ppm and 48–47 ppm, respectively. The succinimide CH<sub>2</sub> groups absorbed at 35–33 ppm and CH<sub>3</sub> lactic acid at 21–16 ppm. The <sup>13</sup>C NMR spectra of ALa and ALt copolymers mainly differ in the CH and CO regions. ALa spectra show intense signals of succinimide CH and CO groups, whereas in ALt spectra, the signals of lactic acid CH and CO groups are predominant.

The differences in the chemical shifts and intensities of signals in the NMR spectra indicate (in accordance with the FTIR spectra) different ratios of aspartic and lactic acid in the copolymers ALa and ALt ( $A/La_L$ ) as compared to the feed ratios. In <sup>1</sup>H NMR spectra of PSL the ratio of CH<sub>2</sub> and CH<sub>3</sub> integrals is equal to  $A/La_L$ . However, the signals of DMSO protons overlap the CH<sub>2</sub> region, so the  $A/La_L$  ratio was approximately (± 10%) estimated from <sup>13</sup>C NMR spectra by integrating the succinimide and lactic acid CH signals (Table 2).

The percentage of end groups in the copolymers, N<sub>C</sub>, (Table 2) was estimated from <sup>1</sup>H NMR spectra with ± 10% precision, due to overlapping signals. The proton sig-

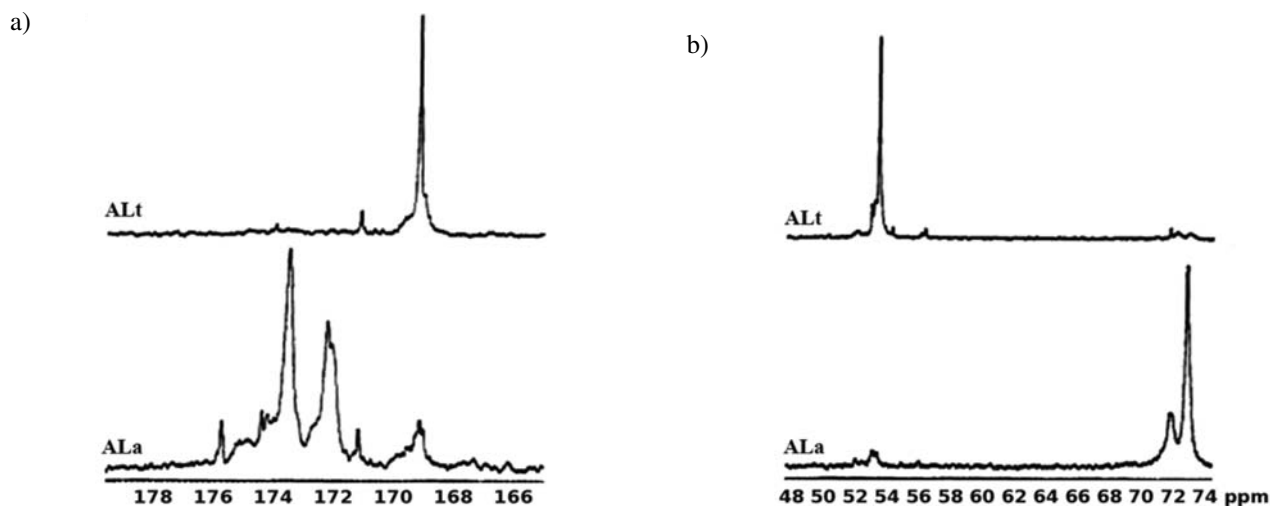


**Figure 1.** <sup>13</sup>C-NMR spectra of PLS ALa and ALt in DMSO-*d*<sub>6</sub>, CO (a) and CH region (b).

nals, representing end units and all comonomer units, were integrated and  $N_C$  was calculated using the equation  $N_C = (a + b + c + d/2) / (f + g + h + d/2)$  (Scheme 1).  $N_C$ , the absolute number average molar mass determined by SEC-MALS,  $M_n$ , and the average molar mass of comonomer units,  $M_{n-unit}$ , were used to calculate the number of end comonomer units per copolymer chain via  $N_{chain} = M_n \cdot N_C / M_{n-unit}$  (Table 2). With  $M_n > 100,000$  g/mol,  $N_C$  from 8 to 9% and  $M_{n-unit}$  from 75 to 90 g/mol, the number of end units per chain was  $> 100$ . More than one hundred end comonomer units per chain indicates a branched copolymer structure.

### 3. 2. Interactions Between Polymer Ligands and $Zn^{2+}$

Fluorescence spectroscopy is a relative method, based upon a calibration curve ( $F^* = f([Zn^{2+}]_t)$ ), where  $F^*$  denotes the relative fluorescence intensity and is calculated via Equation (1). Polymer ligands for binding of  $Zn^{2+}$  ions were PA with 100% aspartic acid units (A), PAL ALa (90% of A) and PAL ALt (10% of A), Table 2.

The fluorescence method was critically evaluated with regard to photobleaching of the indicator FluoZin-1, precision, accuracy, linearity,  $F_{min}$  and  $F_{max}$ . The results indicated no photobleaching of FluoZin-1 over a time period of 300 s, which is long enough to accurately prepare the sample solutions.

The precision of the measurements was tested with preparations in 6 and 4 replicates and measurements of solutions containing 50 and 36  $\mu\text{mol/L}$  free  $Zn^{2+}$  of  $[Zn(ADA)_2]$  solutions, respectively; N-(carbamoylmethyl)iminodiacetic acid buffer (ADA) was used to mimic the conditions in polymer solutions. The error  $dF^*/F^*$  (Equation (3)) was  $\pm 2.5\%$  and the relative standard deviation less than  $\pm 1\%$ . Deviations from the average of duplicate measurements of  $F$  of ZnL solutions showed an accuracy of  $\pm 2.5\%$  (Table A3 in the Supplementary material, column  $[Zn^{2+}]_{f, \text{res}} / \langle [Zn^{2+}]_f \rangle$ ), which is not higher than the  $dF^*/F^*$  error range mentioned above. Therefore the fluorescence measurements were performed at four concentrations of total zinc ions and more than ten concentrations of total polymer ligands in duplicate for each L and the error was attributed to be  $\pm 2.5\%$ .

The accuracy of the proposed method was evaluated by comparing the slopes of the calibration curves from solutions of  $[Zn(ADA)_2]$  with those of  $ZnCl_2$ . With ordinate cross-sections at 0, the slopes of the calibration curves of  $[Zn(ADA)_2]$  and  $ZnCl_2$  were equivalent to 0.041 and 0.036, respectively (Figure 2). With regard to simplified calculations of  $[Zn^{2+}]_f$  in solutions of  $[Zn(ADA)_2]$  (Equation (A1) in the Supplementary material), we consider the slopes to be in good agreement and can be used to calculate total  $Zn^{2+}$  in aqueous copolymer solutions. The solutions of ZnL were therefore prepared without addition of ADA.

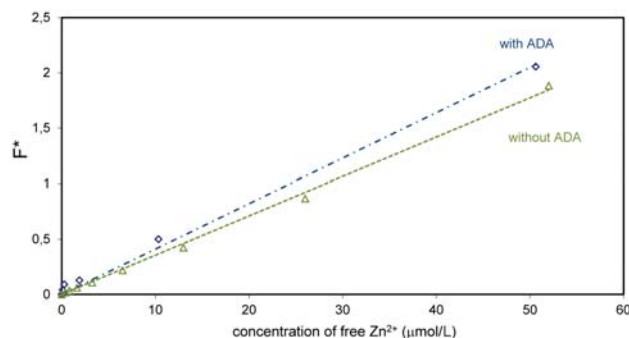


Figure 2. Calibration curves of  $[ZnCl_2]$  and  $[Zn(ADA)_2]$ , pH 6,  $[Zn^{2+}]_f$  0–55  $\mu\text{mol/L}$ .

The deviation from linearity of the calibration curve of  $ZnCl_2$  solutions in the concentration range from 0 to 100  $\mu\text{mol/L}$   $Zn^{2+}$ ,  $R^2$ , was 0.998.  $F_{min}$  and  $F_{max}$  of  $[Zn(ADA)_2]$ ,  $ZnCl_2$  and ZnL solutions were the averages of duplicate measurements of the solutions listed in Table A1 in the Supplementary material. At concentrations higher than 1000  $\mu\text{mol/L}$   $Zn^{2+}$ , small differences in  $F_{max}$  ( $\pm 1\%$ ) produced large errors in calculating  $F^*$  ( $\pm 100\%$ ). To avoid such errors, we prepared samples of ZnL in the concentration range of  $[Zn^{2+}]_t = 20\text{--}80$   $\mu\text{mol/L}$ .

$F_{min}$  and  $F_{max}$  (Table A1 in the Supplementary material), the time dependence of  $F$  (Table A2 in the Supplementary material) and the accuracy of preparing the ZnL solutions (Table A3 in the Supplementary material for PA) were defined.  $F$  values of solutions with constant  $[Zn^{2+}]_t$  (at 20, 40, 60 and 80  $\mu\text{mol/L}$ ) were measured and the values of  $[L]_t$ ,  $F^*$ ,  $[Zn^{2+}]_f$ ,  $[Zn^{2+}]_b$  ( $[Zn^{2+}]_t = [Zn^{2+}]_b + [Zn^{2+}]_f$ ),  $[Zn^{2+}]_b/[Zn^{2+}]_f$  and  $\ln[Zn^{2+}]_f$  were calculated (Table A4 in the Supplementary material for PA). From plots of Type 1 and 2 (Figures 3 and 4) equations for calculating  $Zn^{2+}$  bound to L for any  $[L]_t$  and  $[Zn^{2+}]_t$  (Table 3), and stability constants for binding  $Zn^{2+}$  to L (Table 4) and the concentrations of bound polymer ligands (Table 5) were determined.

24 and 96 hours after the preparation of aqueous solutions of ZnL fluorescence intensities were again measured (Table A2 in the Supplementary material). Due to different voltages in the photomultiplier,  $F$  values of the solutions were not comparable, therefore relative values  $F^*$  were calculated and compared. The results showed substantially more  $Zn^{2+}$  bound to PA 96 hours after preparation of the solutions (smaller values of  $F^*$  after 96 h). The time between preparation of the ZnL solutions and measurement of fluorescence intensity was therefore kept constant, at 96 hours.

In Table 3 the linear equations of Type 1 plots at  $[Zn^{2+}]_t = 40$   $\mu\text{mol/L}$  for all ZnL, together with deviations from linearity,  $R^2$ , are listed.

Figure 3 shows the Type 1 plot at  $[Zn^{2+}]_t$  40  $\mu\text{mol/L}$  for ZnL with PA, PAL ALa and PAL ALt. With  $[L]_t$  5000, the concentration of  $Zn^{2+}$  bound on PA, PAL ALa and PAL ALt is equal to 39, 29 and 11  $\mu\text{mol/L}$ , respectively.

**Table 3.** Dependence of  $[L]_t$  and  $[Zn^{2+}]_f$  at  $[Zn^{2+}]_i = 40 \mu\text{mol/L}$  calculated from *Type 1* plots,  $[L]_t = f(\ln[Zn^{2+}]_f)$  and deviations from linearity,  $R^2$ 

| L        | PA   | PAL ALa   | PAL ALt   |
|----------|--|---|---|
| equation | $[PA]_t = -1438 \cdot \ln[Zn^{2+}]_f + 5347$ | $[PAL ALa]_t = -11940 \cdot \ln[Zn^{2+}]_f + 15275$ | $[PAL ALt]_t = -23650 \cdot \ln[Zn^{2+}]_f + 84280$ |
| $R^2$    | 0.9969                                       | 0.9831  | 0.9894  |
| N        | 11   | 11  | 9   |

N = number of different concentrations of  $[L]_t$

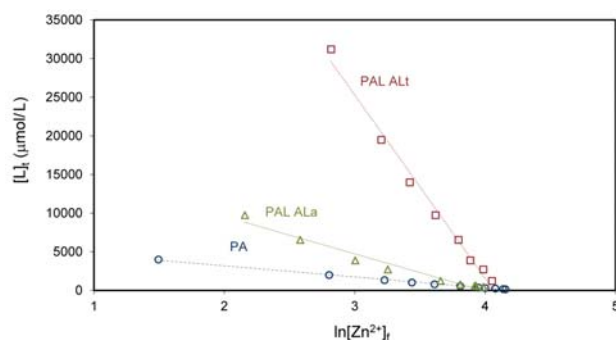
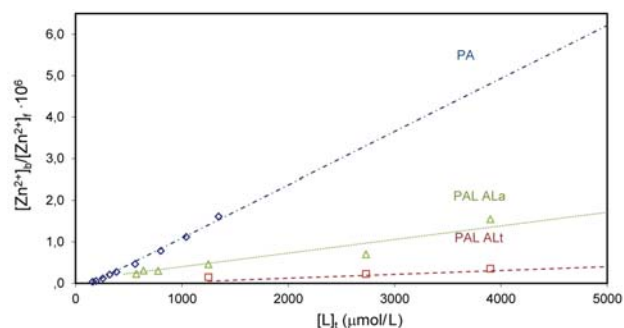
**Figure 3.** *Type 1* plot showing dependence of  $[L]_t$  on  $\ln[Zn^{2+}]_f$ , pH 6,  $[Zn^{2+}]_i = 40 \mu\text{mol/L}$ .**Figure 4.** *Type 2* plot showing dependence of  $[Zn^{2+}]_b/[Zn^{2+}]_f$  on  $[L]_t$ , pH 6,  $[Zn^{2+}]_i = 40 \mu\text{mol/L}$ .

Figure 4 shows the *Type 2* plot for ZnL at  $[Zn^{2+}]_i = 40 \mu\text{mol/L}$ . The straight line can be expressed by the equations  $[Zn^{2+}]_b/[Zn^{2+}]_f = K_L \cdot [L]_t - K_L [L]_b$ . The values in *Type 2* plots at low concentrations of  $[L]_t$  are negative due to the complexity of the calculations, through which experimental errors are summed. Because our main interest was in the slopes of these plots which represent the stability constants for binding of  $Zn^{2+}$  to polymer ligands, these *Type 2* plots are presented without corrections.

**Table 4.** Stability constants of polymer ligands PA, PAL ALa and PAL ALt at pH 6 and  $[Zn^{2+}]_i = 20, 40, 60$  and  $80 \mu\text{mol/L}$  with descriptive statistics – averages (AVG) and relative standard errors (RSE) (determined in fourfold repetition)

| descriptive statistics | PA<br>100% A | PAL ALa<br>90% A | PAL ALt<br>10% A |
|------------------------|--------------|------------------|------------------|
| AVG $K_L$ (L/mol)      | 1445         | 671              | 86               |
| RSE (%)                | 2            | 3                | 8                |

**Table 5.** The concentration of bound polymer ligands,  $[L]_b$ , PA, PAL ALa and PAL ALt, at different  $[Zn^{2+}]_i$  and pH 6 (determined for approx. ten concentrations of total L in duplicate repetition)

| $[Zn^{2+}]_i$ ( $\mu\text{mol/L}$ ) | $[L]_b$ (mmol/L) |                  |                  |
|-------------------------------------|------------------|------------------|------------------|
|                                     | PA<br>100% A     | PAL ALa<br>90% A | PAL ALt<br>10% A |
| 20                                  | 25               | 100              | 510              |
| 40                                  | 145              | 255              | 670              |
| 60                                  | 285              | 600              | 630              |
| 80                                  | 360              | 600              | 670              |

From *Type 2* plots  $K_L$  and  $[L]_b$  were calculated (Tables 4 and 5).

The ability of a polymer ligand to bind a metal ion is dependent on its capacity to donate an electron pair, though this is reduced by steric hindrance<sup>14</sup> such as methyl groups of lactic acid in PAL ALa and PAL ALt, branching of chains and lowering of the molar mass. PA has a  $M_w$  around 3000 g/mol and is approximately linear, whereas PAL ALa and PAL ALt have  $M_w$  around 166,000 and 365,000 g/mol with 140 and 390 end units per chain, respectively; see Table 2. From time dependencies of F values we deduced that PA, PAL ALa and PAL ALt gradually or step-by-step bind  $Zn^{2+}$  (Table A2 in the Supplementary material) and therefore the duration between preparation of the samples and measurement was kept constant.

The interactions between  $Zn^{2+}$  and PA, PAL ALa and PAL ALt were compared by *Type 1* plots (Figure 3 and Table 3), the concentrations of bound L,  $[L]_b$ , and stability constants,  $K_L$  (Tables 4 and 5). With the help of the equations for *Type 1* plots (Table 3) we can relate  $[Zn^{2+}]_t$  and  $[Zn^{2+}]_b$  at constant  $[L]_t$ , and for any  $[Zn^{2+}]_t$  and  $[L]_t$  calculate  $[Zn^{2+}]_b$ . From the linear dependencies in *Type 2* plots (Figure 4) we conclude that zinc ions coordinate on PA, PAL ALa and PAL ALt by the same mechanism, independent of the higher degree of branching in ALa and Alt, and the lower  $M_w$  of PA.

According to Flory's principle,<sup>19</sup> metal ions bind to polymer ligands as if the polymer chains were infinitely long; the reactivity of ligand groups is namely independent of their position on the polymer chain. The binding

of metal ions in this manner is similar to the gradual binding of low molecular weight ligands. Flory's equation for unidentate polymer ligands, our *Type 2* plot, is  $[Zn^{2+}]_b/[Zn^{2+}]_f = K_L \cdot [L]_t - K_L \cdot [L]_b$ . The slope in *Type 2* plots is equal to the product of the stability constant and  $[L]_t$ , and intersect on the ordinate is the product of  $K_L$  and  $[L]_b$ . A lower concentration of bound L indicates a more stable coordination compound and a higher  $K_L$  a higher amount of bound  $Zn^{2+}$  per polymer unit.<sup>14</sup>

$Zn^{2+}$  at pH 6 mainly binds to side groups in polymer ligands.<sup>19,24,25</sup> This means that  $Zn^{2+}$  at pH 6 predominantly binds to carbon of the  $-COO^-$  and  $COOH$  side groups of aspartic acid units of the copolymers of aspartic and lactic acids. The results show that the stability constants for binding of  $Zn^{2+}$  are practically independent of the concentration of total zinc ions (RSE in Table 4), whereas in the curve in Figure 5 they depend on the number of aspartic acid units in the polymer ligand. Namely, PA has 100%, ALa 90% and ALt 10% aspartic acid units and the stability constant for binding of  $Zn^{2+}$  on PA,  $K_{PA}$ , is twice as high as  $K_{PAL,ALa}$  and seventeen-times higher than  $K_{PAL,ALt}$ . The results in Figures 3, 4 and 5 and Table 4 indicate that at pH 6, in comparison to PAL ALa and Alt, PA has the highest capacity for binding of  $Zn^{2+}$ , as expected.

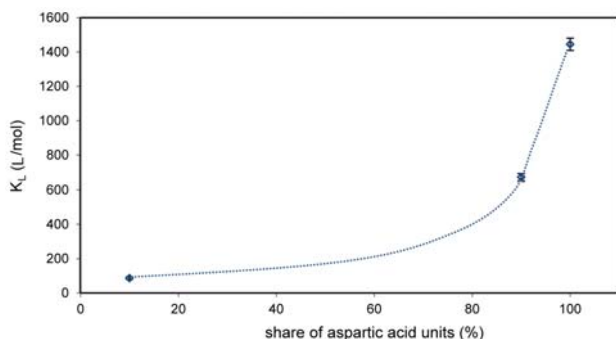


**Figure 5.** Stability constant at pH 6 for binding of  $Zn^{2+}$  on polymer ligands of PA, PAL ALa and PAL ALt (with standard error intervals of fourfold repetition) as a function of aspartic acid moieties in the polymer ligands; PA contains 100%, PAL ALa 90% and PAL ALt 10% of aspartic acid units; the dotted line on the graph is theoretical value.

$[L]_b$  increases with increasing  $[Zn^{2+}]_f$  from 20 to 80  $\mu\text{mol/L}$  (Table 5). The lowest values of  $Zn^{2+}$  bound on polymer ligands are for PA, followed by PAL ALa and PAL Alt, in an increasing order. This could indicate that coordination compounds with PA are the most stable in comparison to PAL ALa and PAL ALt.

In short, the protocol for the method development was as follows:

- determining the fluorescence intensity of the blank ( $F_{\min}$ ) and saturation of the indicator ( $F_{\max}$ ), Table A1, the error of measurements (Equation (3)) and defining the calibration curve – i.e. the re-

lative fluorescence intensity as a function of the concentration of  $Zn^{2+}$ ,  $F^* = f([Zn^{2+}]_f)$ ,

- verifying the potential time dependence of the relative fluorescence intensity  $F^*$  of the polymer coordination compounds (Table A2),
- searching for linear dependences in plots such as for example  $[L]_t = f(\ln[Zn^{2+}]_f)$  and  $[Zn^{2+}]_b/[Zn^{2+}]_f = f([L]_t) = K_L \cdot [L]_t - K_L \cdot [L]_b$ , in order to calculate stability constants of the polymer coordination compounds and the concentration of bound zinc at constant concentrations of total zinc and polymer ligand.

## 4. Conclusions

The products of aspartic and lactic acid or lactide synthesis and basic hydrolysis were poly(succinimide-*co*-lactic acid) and water-soluble poly(sodium  $\alpha,\beta$ -aspartate-*co*-lactic acid), respectively. The average molecular weights ( $M_w$ ) of the copolymers, determined by SEC-MALS, were  $> 100,000$  g/mol. More than 100 end groups per chain were found by  $^1\text{H NMR}$  analysis, indicating the branched structure of the copolymers.

Since the equilibrium of free and bound  $Zn^{2+}$  in aqueous solutions of polymer ligands prevents complete removal of free  $Zn^{2+}$ , interactions between polymer ligands and zinc ions in aqueous solution were followed by a method with fluorescent spectroscopy using the fluorescent indicator dye FluoZin-1 with minimal equilibrium intervention. The protocol is listed in Results and Discussion. By this method we could calculate the stability constants for binding of zinc to the copolymer ligands and furthermore, at constant total ligand and zinc concentrations we could denote the concentration of zinc bound to polymer.

We found that zinc ions gradually or step-by-step bind to the copolymer ligands by the same mechanism, independent of the higher degree of branching in ALa and Alt, and the lower  $M_w$  of PA. With increase of aspartic acid units in the polymer ligands the values of the stability constants increase. Hence, we propose that by modifying the ratio of aspartic acid moieties we can forecast the quantity of coordinated  $Zn^{2+}$ .

## 5. Acknowledgements

The authors gratefully acknowledge Vojmir Francetič for discussions on the behavior of zinc ions in aqueous solutions and the Ministry of Education, Science and Sport of the Republic Slovenia for the financial support.

## 6. References

1. G. Kwon, K. Kataoka, *Adv. Drug Delivery Rev.* **1995**, *16*, 295–309.

2. K. E. Uhrich, S. M. Cannizzaro, R. S. Langer, K. M. Shakesheff, *Chem. Rev.* **1999**, *99*, 3181–3198.
3. K. Tabata, H. Abe, Y. Doi, *Biomacromolecules* **2000**, *1*, 157–161.
4. H. Shinoda, Y. Asou, A. Suetsugu, K. Tanaka, *Macromol. Biosci.* **2003**, *3*, 34–43.
5. J. P. Pennings, H. Dijkstra, A. J. Pennings, *Polymer* **1993**, *34*, 942–951.
6. J. W. Leenslag, A. J. Pennings, R. M. Bos, F. R. Rozema, G. Boering, *Biomaterials* **1987**, *8*, 70–73.
7. K. Makino, M. Arakawa, T. Kondo, *Chem. Pharm. Bull.* **1985**, *33*, 1195–1201.
8. K. Y. Lee, D. J. Mooney, *Chem. Rev.* **2001**, *101*, 1869–1879.
9. S. M. Thombre, B. D. Sarwade, *J. Macromol. Sci., Pure Appl. Chem.* **2005**, *42*, 1299–1315.
10. M. Hershinkel, W. F. Silverman, I. Sekler, *Mol. Med.* **2007**, *13*, 331–336.
11. M. J. Jackson, In: C. F. Mills (Ed.), *Zinc in human biology*, Springer-Verlag, London, **1989**, pp. 1–14.
12. J. C. King, D. M. Shames, L. R. Woodhouse, *J. Nutr.* **2000**, *130*, 1360S–1366S.
13. D. Wöhrle, A. D. Pomogailo, In: H. S. Nalwa (Ed.), *Advanced Functional Molecules and Polymers*, Overseas Publishers Association, **2001**, *1*, pp. 87–161.
14. F. Ciardelli, E. Tsuchida, D. Wöhrle, A. D. Pomogailo, *Macromolecule-Metal Complexes*, Springer, **1996**, pp. 1–112.
15. V. Saudek, Š. Štokrova, P. Schmidt, *Biopolymers* **1982**, *21*, 1011–1020.
16. M. Gričar, I. Poljanšek, B. Brulc, T. Šmigovec, M. Žigon, E. Žagar, *Acta Chim. Slov.* **2008**, *55*, 575–581.
17. M. Gričar, M. Žigon, E. Žagar, *Anal. Bioanal. Chem.* **2009**, *393*, 1815–1823.
18. B. L. Rivas, E. D. Pereira, I. M. –Villoslada, *Prog. Polym. Sci.* **2003**, *28*, 173–208.
19. A. D. Pomogailo, I. E. Uflyand, *Adv. Polym. Sci.* **1990**, *97*, 61–105.
20. T. Nakato, M. Yoshitake, K. Matsubara, M. Tomida, *Macromolecules* **1998**, *31*, 2107–2113.
21. K. Matsubara, T. Nakato, M. Tomida, *Macromolecules* **1998**, *31*, 1466–1472.
22. K. Matsubara, T. Nakato, M. Tomida, *Macromolecules* **1997**, *30*, 2305–2312.
23. J. L. Espartero, L. Rashkov, S. M. Li, N. Manolova, M. Vert, *Macromolecules* **1996**, *29*, 3535–3539.
24. R. Nakon, C. R. Krishnamoorthy, *Science* **1983**, *221*, 749–750.
25. E. A. Lance, R. Nakon, *Inorg. Chim. Acta* **1981**, *55*, L1–L3.

## Povzetek

Sintetizirali smo biorazgradljive kopolimere asparaginske in mlečne kisline, ki imajo možno uporabo kot nosilci za nadzirano sproščanje zdravilnih učinkovin. Molekule kopolimerov so bile razvejene, z absolutnimi molskimi masami nad 100.000 g/mol in deležem enot asparaginske kisline 0,9 ter 0,1. Za vezavo zdravilne učinkovine na kopolimere bi lahko uporabili komplekse s kovinskimi (predvsem cinkovimi) ioni, zato smo za opredelitev interakcij med cinkovimi ioni in polimernimi ligandi razvili metodo za določanje prostih cinkovih ionov v vodnih raztopinah polimerov s fluorescenčno spektroskopijo. Določili smo stabilnostne konstante vezave cinka in koncentracije vezanega cinka. Ugotovili smo, da se cinkovi ioni pri pH 6 vežejo predvsem na asparaginske enote kopolimerov asparaginske in mlečne kisline.

## SUPPLEMENTARY MATERIAL

### Calibration and method development for determination of interactions between polymer ligands and Zn<sup>2+</sup> by fluorescence spectroscopy

#### 1. Method

Calibration curves of solutions of ZnCl<sub>2</sub> + ADA and ZnCl<sub>2</sub> were plotted at pH 6 and their slopes compared. At pH values higher than 6.3, free Zn<sup>2+</sup> in aqueous solution is unstable due to precipitation [A1]. In ZnCl<sub>2</sub> + ADA solutions at pH 6 two complexes, [Zn(ADA)<sub>2</sub>] and [Zn(ADA)], are formed, but, [Zn(ADA)<sub>2</sub>] highly predominates [A2-A4]. [Zn<sup>2+</sup>]<sub>f</sub> in solutions of ZnCl<sub>2</sub> + ADA can therefore be simply calculated by Equation (A1), using the stability constant of [Zn(ADA)] ( $K_{[Zn(ADA)]} = 127$  nmol/L, when Zn<sup>2+</sup> : ADA = 1 : 1), considering twice as

much free Zn<sup>2+</sup> in solutions of [Zn(ADA)<sub>2</sub>] than [Zn(ADA)] and 50% dilution with Milli-Q water in the cuvette; “<sub>t</sub>” denotes total:

$$[Zn^{2+}]_f = 0.5 [Zn^{2+}]_t - 0.5 [ADA]_t - K_{ZnADA} + \quad (A1)$$

$$\frac{[(0.5 [Zn^{2+}]_t - 0.5 [ADA]_t - K_{ZnADA})^2 + 2 K_{ZnADA} [Zn^{2+}]_t]^{1/2}}$$

#### 2. Results

**Table A1.** F<sub>min</sub> and F<sub>max</sub> of [Zn(ADA)<sub>2</sub>], ZnCl<sub>2</sub> and ZnL solutions at pH 6

| solution                                 | [Zn(ADA) <sub>2</sub> ] |                  | ZnCl <sub>2</sub> |                  | ZnL              |                  |
|--|-------------------------|------------------|-------------------|------------------|------------------|------------------|
|  | F <sub>min</sub>        | F <sub>max</sub> | F <sub>min</sub>  | F <sub>max</sub> | F <sub>min</sub> | F <sub>max</sub> |
| [ADA] <sub>t</sub> (mol/L)               | 0.05215                 | 0.04736          | –                 | –                | –                | –                |
| [Zn <sup>2+</sup> ] <sub>t</sub> (mol/L) | 0                       | 0.04867          | 0                 | 0.052            | 0                | 0.052            |
| [Zn <sup>2+</sup> ] <sub>f</sub> (mol/L) | 0                       | 0.0026           | 0                 | 0.052            | 0                | 0.052            |
| [NaCl] (mol/L)                           | 0.048                   | 0.09             | 0.1               | 0.048            | 0.1              | 0.048            |
| [L] <sub>t</sub> (mol/L)                 | –                       | –                | –                 | –                | max              | 0                |

**Table A2.** Fluorescence intensities (F) 24 and 96 hours after the preparation of solutions at pH 6, and relative F (F\*) and F\* ratios

| [Zn <sup>2+</sup> ] <sub>t</sub><br>(μmol/L) | [PA] <sub>t</sub><br>(μmol/L) | [Zn <sup>2+</sup> ] <sub>t</sub> /[PA] <sub>t</sub> (l) | F (rlu) |      | F*               |                  | F* <sub>(24 h)</sub> /F* <sub>(96 h)</sub><br>(%) |
|--|-------------------------------|---|---------|------|------------------|------------------|---|
|  |                               |   | 24 h    | 96 h | 24 h             | 96 h             |   |
| 11250  | 500                           | 22.5  | 336     | 515  | 24               | 13               | 185   |
| 10000  | 500                           | 20  | 329     | 500  | 15               | 9                | 167   |
| 125  | 500                           | 0.25  | 266     | /    | 3                | /                | /   |
| 50   | 500                           | 0.1   | 231     | 316  | 1.6              | 1.1              | 145   |
| 4  | 500                           | 0.008   | 51      | 70   | 0.05             | 0.03             | 167   |
| 2  | 500                           | 0.004   | 40      | /    | 0.01             | /                | /   |
| 0.8  | 500                           | 0.002   | 40      | 57   | 0.01             | 0                | /   |
| 0  | 500                           | 0   | 38      | 58   | F <sub>min</sub> | F <sub>min</sub> | F <sub>min</sub>                                  |
| 52000  | 0                             | /   | 349     | 549  | F <sub>max</sub> | F <sub>max</sub> | F <sub>max</sub>                                  |

**Table A3.**  $[\text{Zn}^{2+}]_t$  40, 60 and 80  $\mu\text{mol/L}$ , 96 hours after the preparation of solutions of  $\text{ZnCl}_2 + \text{PA}$ , pH 6: average  $F^*$  ( $\langle F^* \rangle$ ), deviation from average  $F^*$  ( $F^* - \langle F^* \rangle$ ), average  $[\text{Zn}^{2+}]_f$  of duplicates ( $\langle [\text{Zn}^{2+}]_f \rangle$ ), deviation from average ( $[\text{Zn}^{2+}]_{f^{**}}$ ) and ratio between  $[\text{Zn}^{2+}]_{f^{**}}$  and  $\langle [\text{Zn}^{2+}]_f \rangle$ 

| $[\text{Zn}^{2+}]_t$<br>( $\mu\text{mol/L}$ ) | $[\text{PA}]_t$<br>( $\mu\text{mol/L}$ ) | $[\text{Zn}^{2+}]_t/[\text{PA}]_t$<br>(/) | $\langle F^* \rangle$ | $F^* - \langle F^* \rangle$ | $\langle [\text{Zn}^{2+}]_f \rangle$<br>( $\mu\text{mol/L}$ ) | $[\text{Zn}^{2+}]_{f^{**}}$<br>( $\mu\text{mol/L}$ ) | $[\text{Zn}^{2+}]_{f^{**}}/\langle [\text{Zn}^{2+}]_f \rangle$<br>(%) |
|---|--|---|-----------------------|-----------------------------|---|--|---|
| 40  | 16                                       | 2.5                                       | 1.65                  | 0.03                        | 46  | 0.7  | 1.5   |
| 40  | 64                                       | 0.63                                      | 1.52                  | 0.03                        | 42.5  | 0.6  | 1.5   |
| 40  | 128                                      | 0.31                                      | 1.44                  | 0.03                        | 40  | 0.6  | 1.4   |
| 40  | 160                                      | 0.25                                      | 1.38                  | 0.02                        | 39  | 0.5  | 1.4   |
| 40  | 192                                      | 0.21                                      | 1.35                  | 0.02                        | 38  | 0.5  | 1.4   |
| 40  | 256                                      | 0.16                                      | 1.28                  | 0.03                        | 36  | 0.7  | 1.9   |
| 40  | 320                                      | 0.13                                      | 1.18                  | 0.03                        | 33  | 0.7  | 2.1   |
| 40  | 384                                      | 0.10                                      | 1.12                  | 0.02                        | 31  | 0.4  | 1.3   |
| 40  | 1344                                     | 0.03                                      | 0.55                  | 0.01                        | 15  | 0.1  | 0.8   |
| 40  | 4000                                     | 0.01                                      | 0.10                  | 0.00                        | 3   | 0.0  | 0.1   |
| 40  | 6400                                     | 0.006                                     | 0.03                  | 0.00                        | 0.8   | 0.0  | 1.1   |
| 60  | 384                                      | 0.16                                      | 1.74                  | 0.02                        | 48  | 0.3  | 0.6   |
| 60  | 480                                      | 0.13                                      | 1.59                  | 0.00                        | 45  | 0.2  | 0.5   |
| 60  | 576                                      | 0.10                                      | 1.49                  | 0.03                        | 42  | 0.6  | 1.4   |
| 80  | 512                                      | 0.16                                      | 2.20                  | 0.05                        | 61.5  | 1.1  | 1.8   |
| 80  | 640                                      | 0.13                                      | 1.97                  | 0.06                        | 55  | 1.4  | 2.5   |
| 80  | 768                                      | 0.10                                      | 1.83                  | 0.05                        | 51  | 1.1  | 2.1   |
| 0   | 6400                                     | 0   | $F_{\min}$            | $F_{\min}$                  | /   | /  | /   |
| 52000   | 0  | /   | $F_{\max}$            | $F_{\max}$                  | /   | /  | /   |

$$F_1^* = (F_1 - 15) / (415 - F_1), F_2^* = (F_2 - 15) / (415 - F_2), \text{ calibration curve: } [\text{Zn}^{2+}]_f = 28 \cdot F$$

**Table A4.** Solutions of  $[\text{Zn}^{2+}]_t$  40  $\mu\text{mol/L}$  and different concentrations of total PA, pH 6, 96 hours after preparation of the solutions: F and  $F^*$ , concentrations of free  $\text{Zn}^{2+}$ , natural logarithm of free  $\text{Zn}^{2+}$  and ratio between bound and free  $\text{Zn}^{2+}$ 

| $[\text{Zn}^{2+}]_t$<br>( $\mu\text{mol/L}$ ) | $[\text{PA}]_t$<br>( $\mu\text{mol/L}$ ) | $[\text{Zn}^{2+}]_t/[\text{PA}]_t$ | F (rtu) | $F^*$             | $[\text{Zn}^{2+}]_f$<br>( $\mu\text{mol/L}$ ) | $\ln[\text{Zn}^{2+}]_f$ | $[\text{Zn}^{2+}]_b/[\text{Zn}^{2+}]_f$ |
|---|--|------------------------------------|---------|-------------------|---|-------------------------|---|
| 40  | 16                                       | 2.50                               | 264     | 1.65 <sup>a</sup> | 46  | 3.84                    | -0.14                                   |
| 40  | 65                                       | 0.63                               | 256     | 1.52 <sup>a</sup> | 42.5  | 3.75                    | -0.06                                   |
| 40  | 130                                      | 0.31                               | 251     | 1.44 <sup>a</sup> | 40  | 3.70                    | -0.01                                   |
| 40  | 160                                      | 0.25                               | 247     | 1.38 <sup>a</sup> | 39  | 3.66                    | 0.03                                    |
| 40  | 190                                      | 0.21                               | 245     | 1.35 <sup>a</sup> | 38  | 3.64                    | 0.05                                    |
| 40  | 260                                      | 0.16                               | 239     | 1.28 <sup>a</sup> | 36  | 3.58                    | 0.12                                    |
| 40  | 320                                      | 0.13                               | 231     | 1.18 <sup>a</sup> | 33  | 3.50                    | 0.21                                    |
| 40  | 380                                      | 0.10                               | 226     | 1.12 <sup>a</sup> | 31  | 3.45                    | 0.27                                    |
| 40  | 560                                      | 0.07                               | 232     | 0.92 <sup>b</sup> | 27  | 3.31                    | 0.46                                    |
| 40  | 800                                      | 0.05                               | 210     | 0.76 <sup>b</sup> | 22  | 3.11                    | 0.78                                    |
| 40  | 1040                                     | 0.04                               | 191     | 0.64 <sup>b</sup> | 19  | 2.94                    | 1.12                                    |
| 40  | 1344                                     | 0.03                               | 155     | 0.54 <sup>a</sup> | 15  | 2.73                    | 1.61                                    |
| 40  | 2000                                     | 0.02                               | 129     | 0.34 <sup>b</sup> | 10  | 2.30                    | 3.00                                    |
| 40  | 4000                                     | 0.01                               | 50      | 0.10 <sup>a</sup> | 3   | 0.99                    | 13.81                                   |
| 40  | 6400                                     | 0.01                               | 26      | 0.03 <sup>a</sup> | 0.8   | -0.22                   | 49.00                                   |
| 52000   | 0  | /                                  | 415     | $F_{\max}^a$      | /   | /                       | /                                       |
| 52000   | 0  | /                                  | 468     | $F_{\max}^b$      | /   | /                       | /                                       |
| 0   | 6400                                     | 0                                  | 15      | $F_{\min}^a$      | 0   | /                       | /                                       |
| 0   | 6400                                     | 0                                  | 15      | $F_{\min}^b$      | 0   | /                       | /                                       |

$$^a: F^* = (F - 15) / (415 - F), [\text{Zn}^{2+}]_f = 28 \cdot F^*; \quad ^b: F^* = (F - 15) / (468 - F), [\text{Zn}^{2+}]_f = 30 \cdot F^*$$

The measurements F in Table A4 differ in their date of measurement, which is denoted with <sup>“a”</sup> and <sup>“b”</sup>.

### 3. References

- A1. F. Caillaud, A. Smith, J.-F. Baumard, *J. Am. Ceram. Soc.* **1993**, 76, 998–1002.
- A2. E. A. Lance, C. W. Rhodes, III, R. Nakon, *Anal. Biochem.* **1983**, 133, 492–501.
- A3. R. Nakon, C. R. Krishnamoorthy, *Science* **1983**, 221, 749–750.
- A4. E. A. Lance, R. Nakon, *Inorg. Chim. Acta* **1981**, 55, L1–L3.